Guojun Wang
State Key Laboratory of Space Weather, National Space Science Center, Chinese Academy of Sciences,
Address: No.1 Zhongguancun nanertiao, Haidian District, Beijing, China, 100190.
Email: gjwang@nssc.ac.cn

Jiankui Shi
State Key Laboratory of Space Weather, National Space Science Center, Chinese Academy of Sciences,
Address: No.1 Zhongguancun nanertiao, Haidian District, Beijing, China, 100190.
Email: jkshi@nssc.ac.cn

Zheng Wang
State Key Laboratory of Space Weather, National Space Science Center, Chinese Academy of Sciences,
Address: No.1 Zhongguancun nanertiao, Haidian District, Beijing, China, 100190.
Email: zwang@spaceweather.ac.cn

Xiao Wang
State Key Laboratory of Space Weather, National Space Science Center, Chinese Academy of Sciences,
Address: No.1 Zhongguancun nanertiao, Haidian District, Beijing, China, 100190.
Email: wangx@nssc.ac.cn

Elena Romanova
Institute of Solar-Terrestrial Physics, Russian Academy of Sciences, Irkutsk, 664033, Russia
Address: Lermontov st., 126a, Irkutsk, Russia
Email: ebr@iszf.irk.ru

Konstantin Ratovsky
Institute of Solar-Terrestrial Physics, Russian Academy of Sciences, Irkutsk, 664033, Russia
Address: Lermontov st., 126a, Irkutsk, Russia
Email: Ratovsky@iszf.irk.ru

Nelia Mikhailovna Polekh
Institute of Solar-Terrestrial Physics, Russian Academy of Sciences, Irkutsk, 664033, Russia
Address: Lermontov st., 126a, Irkutsk, Russia
Email: Polekh@iszf.irk.ru

Solar cycle variation of ionospheric parameters over the low latitude station Hainan, China, during 2002-2012 and its comparison with IRI -2012 model

G. J. Wang[1], J. K. Shi[1,2], Z. Wang[1], X. Wang[1], E. Romanova[3], K. Ratovsky[3], N. M. Polekh[3]

[1]State Key Laboratory of Space Weather, National Space Science Center, Chinese Academy of Sciences, Beijing, 100190, China
[2]University of Chinese Academy of Sciences, Beijing, 100049, China
[3]Institute of Solar-Terrestrial Physics, Russian Academy of Sciences, Irkutsk, 664033, Russia

Abstract. The low latitude ionospheric data observed by digisonde at Hainan station (19.5º N, 109.1º E) in a whole solar activity cycle period from 2002 to 2012 within Ap<20 have been analyzed to explore the diurnal, seasonal, annual variations and solar activity dependences of the ionospheric peak parameters (foF2, hmF2, and Chapman scale height Hm), as well as some quantitative comparison with IRI-2012 modeling predictions. The results show that the winter anomaly in the daytime foF2 appears at different levels of solar activity. The semiannual anomaly in the daytime and nighttime foF2 with two maxima in equinox seasons is present. The foF2 have a close correlation with a solar activity factor F107P = (F107+F107A)/2 and the correlation coefficients (r) in their diurnal variation are around 0.7. The slope of foF2 varying with F107P in daytime is usually smaller than in nighttime. The afternoon and evening hmF2 show good correlation with F107P (their r values exceed 0.6), but hmF2 at other time are low or poor related to F107P. The prominent character of hmF2 in equinox and summer seasons is its strong increase at sunset in high solar activity period, which may be due to pre-reversal enhancement (PRE) of local electric field. We also note that hmF2 values around midnight slightly decrease with increasing F107P index in equinox seasons. The diurnal variation of Hm usually has two peaks around noontime and pre-sunrise. The daytime Hm has an annual variation with maximum in summer and minimum in winter. Moreover, the dependence of the daytime Hm on solar activity is not strong due to meridional wind and other factors. The above results over Hainan are considerably different from those reported over Millstone Hill, which is attributed to their different geomagnetic locations. The quantitative results compared between IRI-2012 model predictions and observations show that the predicted foF2 values are basically underestimated and the magnitude of their deviations obviously increases with increasing solar activity. The predicted hmF2 obtained with measured M(3000)F2 inputs in low and moderate solar activity agree well with the observed ones. However, their deviations in high solar activity are significantly magnified.

Keywords: ionospheric peak parameters, low latitude ionosphere, IRI-2012 model

1. Introduction

The ionospheric F2 layer critical frequency foF2, the peak height hmF2, and the corresponding scale height are very important parameters for ionospheric studies and empirical modeling as well as for associated practical applications. These parameters describing the ionospheric characteristics exhibit significant variations with solar activity, geomagnetic activity, season, and local time, which are due to solar extreme ultraviolet (EUV) and X-ray radiations disturbance or various chemical and dynamic processes (e.g., Torr and Torr, 1973; Kane, 1992; Balan et al., 1994a, 1994b; Richards et al., 1994; Rishbeth, 1998, 2000a, 2000b; Richards, 2001; Kawamura et al., 2002; Laštovička, 2006). Although these ionospheric parameters have been studied for several decades, there are still some questions about them not fully resolved, for example, their annual and semiannual variations of equatorial ionosphere (Rishbeth, 2004). It is therefore necessary to continue to conduct some investigations in the variations of these ionospheric parameters to provide not only a fuller understanding of the ionospheric physical mechanisms but also more accurate ionospheric models for related forecasting applications.

In the last few decades there have been plenty of studies on the variations of ionospheric F2 peak parameters based on the observations by different instruments, such as ionosonde, incoherent scatter radar (ISR), and satellite radio occultation, as well as by model computations (e.g., Adler et al., 1997; Balan et al., 1994a; Kane, 1992; Mikhailov and Mikhailov, 1995; Millward et al., 1996; Zou et al., 2000; Richards, 2001; Yu et al., 2004; Lei et al., 2005; Liu et al., 2006a, 2006b, 2007, 2008; Lee and Reinisch, 2006, 2007; Nambala et al., 2008; Ratovsky et al., 2009; Mosert et al., 2012; Rao et al., 2014; Haralambous and Oikonomou, 2015). For example, using the long-term data obtained by ionosonde and ISR over the middle latitude station Millstone Hill (42.6º N, 288.5º E), Lei et al. (2005) have studied the ionospheric peak parameters during low geomagnetic activity. They indicated that NmF2 and hmF2 increase with daily F107 index and saturate (or increase with a much lower rate) for very high F107; but they are almost linearly dependent on the solar proxy index F107P = (F107 +F107A)/2, where F107A is the 81-day running mean of daily F107. Lee and Reinisch (2006) utilized the measurements of the digisonde at Jicamarca station (12º S, 76.9º W) to examine the variations in F2 layer peak electron density (NmF2), its height (hmF2), and the F2 layer thickness parameter (B0) near the dip equator during the maximum solar activity. They have showed that higher hmF2 values during daytime, associated with the upward velocity, are mainly responsible for the greater NmF2 and B0; while the nighttime hmF2 associated with the downward velocity are mainly responsible for the smaller NmF2 and B0. Liu et al (2007) reported the diurnal and seasonal variations of scale height in the lower topside ionosphere based on the Arecibo (18.3º N, 293.2º E) incoherent scatter radar measurements, and confirmed the sensitivity of ionospheric scale height to thermal structure and dynamics. Recently, Rao et al. (2014) used ionosonde data over a mid latitude station Novosibirsk (54.6º N, 83.2º E) to analyze the variations of monthly mean foF2 and hmF2 during the period 1997-2006, as well as to compare their results with the International Reference Ionosphere (IRI) model predictions (Bilitza and Reinisch, 2008). They showed the presence of winter anomaly and semiannual anomaly in the daily foF2 during different phases of solar activity, and pointed out that IRI model predictions on foF2 and hmF2 during equinoxes differ significantly from the observations.

As mentioned above, considerable progress has been made in understanding the diurnal,

seasonal, annual and solar cycle variations of ionospheric peak parameters. However, most of these studies focus on the mid-latitude region or near dip equator [e.g., Rao, et al., 2014; Lee and Reinisch, 2006], and there are few analyses applied to the transition region from the equatorial ionization anomaly to dip equator, especially in East Asia area. In the transition region, the ionospheric peak parameters, as compared with those over other latitude regions, are peculiar due to the small inclination configuration of geomagnetic field lines. The little oblique field assists in forming the vertical plasma motions controlled by the zonal electric fields and meridional winds (Abdu, 2005). Hainan station (19.5º N, 109.1º E, Mag. Lat. 9.0º N, Dip: 22º) just situated on south side of north equatorial ionization anomaly (EIA). Previous studies based on observations over Hainan only for two years or declining phase in the 23rd solar cycle have demonstrated some results on the diurnal and seasonal variations of foF2, hmF2, and Chapman scale height Hm, as well as preliminary comparison with IRI model (Zhang et al, 2004, 2006, 2007; Wang et al, 2009). However, the understanding of the behavior of the peak parameters for a longer period like a solar cycle over Hainan has not been done yet.

This paper extends previous works to examine the variations of peak parameters in detail. The objective of this paper is to analyze foF2, hmF2, and Hm (Chapman scale Height at F2 peak) results from a carefully manual scaled DPS-4 digisonde dataset over Hainan station covering a solar cycle (2002-2012) during low to moderate geomagnetic activity period. In the following sections, we first describe our measurements and methodology, then present the diurnal, seasonal variations and solar activity dependence of the three parameters, and some comparisons between IRI-2012 predictions and our results as well. In section 4 the summary is given. These results might be valuable for the improvement of IRI over the low latitude region near Southeast Asia.

2. Data and Method

The data used for the present study are the 15-min values of foF2, hmF2, and Hm obtained from the ionograms for the period from 2002 to 2012, covering a solar activity cycle. All these parameters are scaled or deduced from manually edited ionograms recorded by DPS-4 digisonde over Hainan station. The main absent periods of the data due to instrument failure are from 254 to 315 (Day of year) in 2005, from 327 in 2009 to 70 in 2010, and from 300 to 315 in 2010. The total absent data percentage is less than 5%. The DPS-4 data have been grouped into four seasonal bins: the winter season includes January, February, November, December; the spring season includes March, April; the summer season includes May, June, July, August; the autumn season includes September and October. We also divide the data according to low (F107A $\leq$100), moderate (100 < F107A $\leq$150) and high (F107A >150) solar activity levels (Lei et al., 2005). To minimize the effects of geomagnetic activity, the data are selected with 3-hourly Ap <20 (corresponding to low to moderate geomagnetic activity conditions). The F107 and Ap indices data are downloaded from Space Physics Interactive Data Resource (SPIDR).

Besides F107 index, which is regarded as the scaling factor of solar activity, a solar activity factor F107P, i.e., F107P= (F107 +F107A)/2, can also be taken as the scaling factor solar activity (e.g., Hinteregger et al., 1981). Figure 1 illustrates that the daily variations of F107 and F107P during the period from 2002 to 2012, and the monthly observation numbers of each parameter over Hainan station under geomagnetic condition Ap<20, which are divided by 100. It is obvious

that the days in high solar activity are less than those in low or moderate solar activity. In fact, the days in high solar activity are about 354 days (~ 34,000 ionograms) and total number of ionograms used is about 242,000.

Since 2008-2009 period is extremely low solar activity period, quality of the ionograms in the late night is very poor at many places across the globe due to low ionospheric densities. It is also poor over Hainan before the dawn (usually during 0300-0500 LT), mainly in winter months. The ionograms with foF2 values lower than the starting scan frequency of digisonde (1.5 MHz in 2008 and 1 MHz since 2009) are remarked as defect observation event. Statistically, the ratio of such defect ionograms to all recorded ionograms during 0000-0600 LT in 2008 is about 20%. However, the ratio in 2009 is very small and less than 1%. In total, during the extremely low solar activity periods, the ionograms data recorded at Hainan station before the dawn will be used carefully.

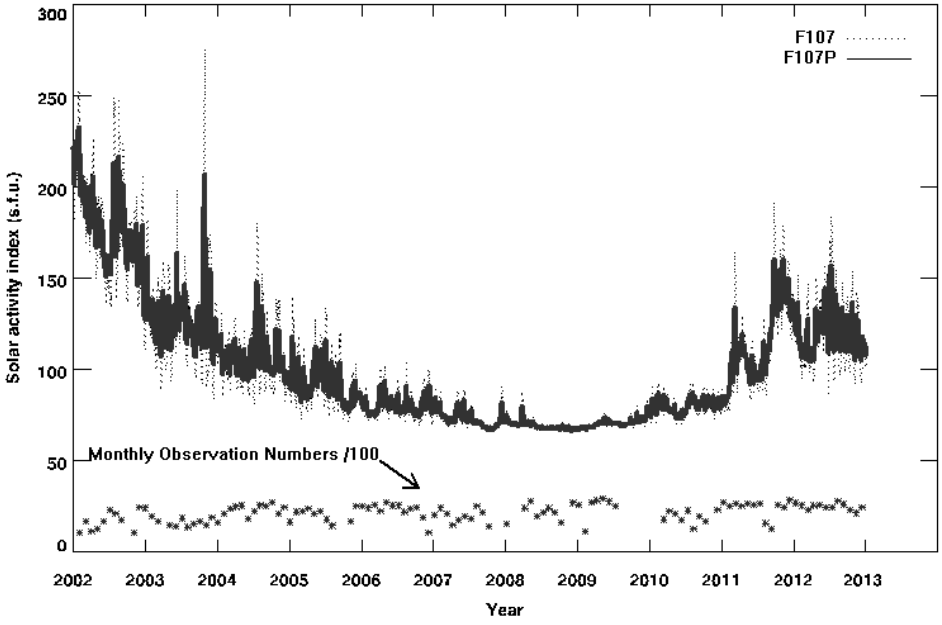

Figure 1. The daily variations of solar activity index F107 and F107P from 2002 to 2012 are depicted by dotted line and solid line, respectively. The monthly observation numbers of each parameter obtained at Hainan station under geomagnetic condition Ap <20 are illustrated by star symbol in the bottom of figure, but divided by 100. The solar flux index unit is 10^{-22} W m^{-2} Hz^{-1} (s.f.u.).

3. Results and discussion

3.1 foF2 Morphology

Figure 2 shows the diurnal and seasonal variation of median foF2 under low, moderate, and high solar activity. Notice that the local time of Hainan is LT= UT+7.3h. For low solar activity, the diurnal variations of foF2 in four seasons have a similar trend, i.e. after a sharp increase starting from around 0500 LT, foF2 gradually reaches its diurnal peak around noon, then decreases until dawn. The diurnal peak of foF2 in different seasons occurs at different local time, it occurs around 1500 LT in spring and autumn but around 1300 LT in winter and around 1600 LT in summer. In daytime and nighttime, the foF2 in equinox seasons (autumn and spring) are higher than that in

solstice seasons (winter and summer), which are manifestation of the semiannual anomaly. Furthermore, the daytime foF2 in spring is basically larger than that in autumn. Overall, the daytime foF2 is highest in spring and lowest in summer, while during nighttime it is still the highest in spring but the lowest in winter. The well-known winter anomaly is confirmed by comparing the higher foF2 values in winter with the lower ones in summer during 0900-1500 LT. For moderate and high solar activity, the diurnal and seasonal variations are generally similar to those under low solar activity, but they have considerable differences in detail. The winter anomaly is also pronounced and the daytime peak values of foF2 in each season become much larger. It is interesting to note that the duration of the adjacent values around daytime peak of foF2 in each season are prominently extended especially in high solar activity. The semiannual anomaly turns out to be weak in high solar activity. Over Hainan station, as the green shade shown in Figure 2, the winter anomaly of foF2 is clearly present in all years, whereas semiannual variations of foF2 are significant in low and moderate solar activity, and weak in high solar activity. Previous studies have indicated that both the winter anomaly and semiannual variations of foF2 are mainly related to the variation of the ratio of atomic oxygen to molecular nitrogen [O/N2], which is usually attributed to wind patterns and their stirred effects in different seasons (Rishbeth and Setty, 1961; Fuller-Rowell, 1998; Qian et al., 2013). Furthermore, the semiannual variation of the diurnal tide in the lower thermosphere induces the semiannual variation of foF2 over low latitude region through the equatorial fountain effect (Ma et al., 2003). So the above two mechanisms would be reasonable to have crucial influences on seasonal variations of foF2 over Hainan. In addition, the factors causing the semiannual variation of foF2 over Hainan weak in high solar activity are not clear, and this issue needs to be investigated further.

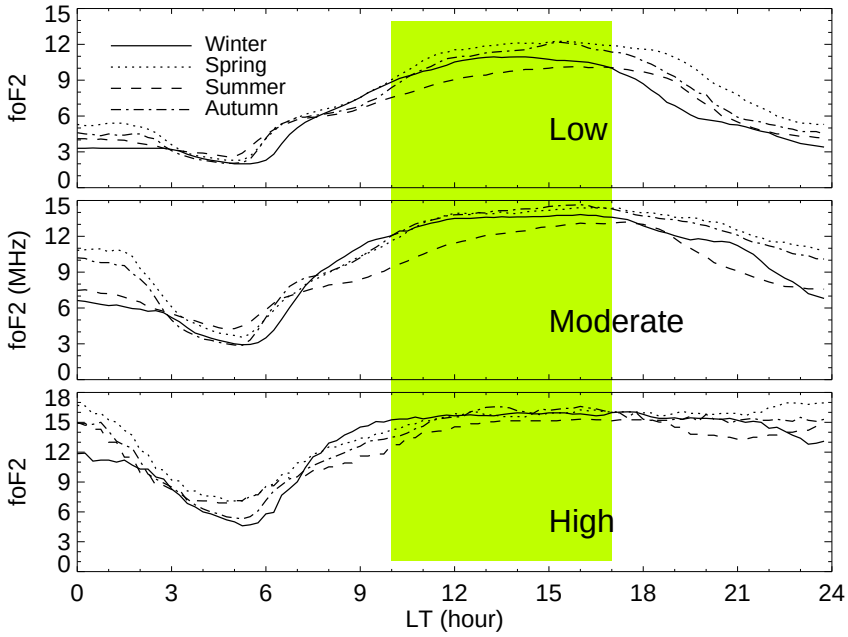

Figure 2. The diurnal and seasonal variation of median foF2 under low, moderate, and high solar activities over Hainan, and the green shade shows the local time of winter and semiannual anomaly.

With regard to the solar activity dependence, Figure 3 shows the responses of all observed foF2 at 1200 LT to daily F107 index and F107P. Here solar flux indices F107 and F107P are in

unit of 10^{-22} W m^{-2} Hz^{-1} (s.f.u.). The fitted curves represent the linear and 2nd degree polynomials fitting for the data. We can see from Figure 3 (top) that the foF2 increases with daily F107 when daily F107 is less than 180, but it begins to decrease when daily F107 is greater than 180. This saturated feature is reported by some previous studies. In particular, Lei et al. (2005) comprehensively analyzed the solar cycle variation of ionospheric peak parameters obtained by ionosonde and incoherent scatter radar (ISR) over Millstone Hill for the period 1976-2002, hence we have an opportunity to do some comparison of our results with their observations to show the ionospheric regional characters on the solar cycle variation of peak parameters over the low latitude station Hainan and middle latitude station Millstone Hill in the following section. Here, they found the NmF2 over Millstone Hill follows the saturation feature for high F107 index. Whereas, it can be seen in Figure 3 (bottom) that observed foF2 increase linearly with increasing solar activity index F107P. Comparing the Figure 3 top and bottom, we found that the linear dependence between foF2 and F107P is more distinct than that between foF2 and F107. Therefore F107P will be taken as an indicator of solar activity in the following analysis.

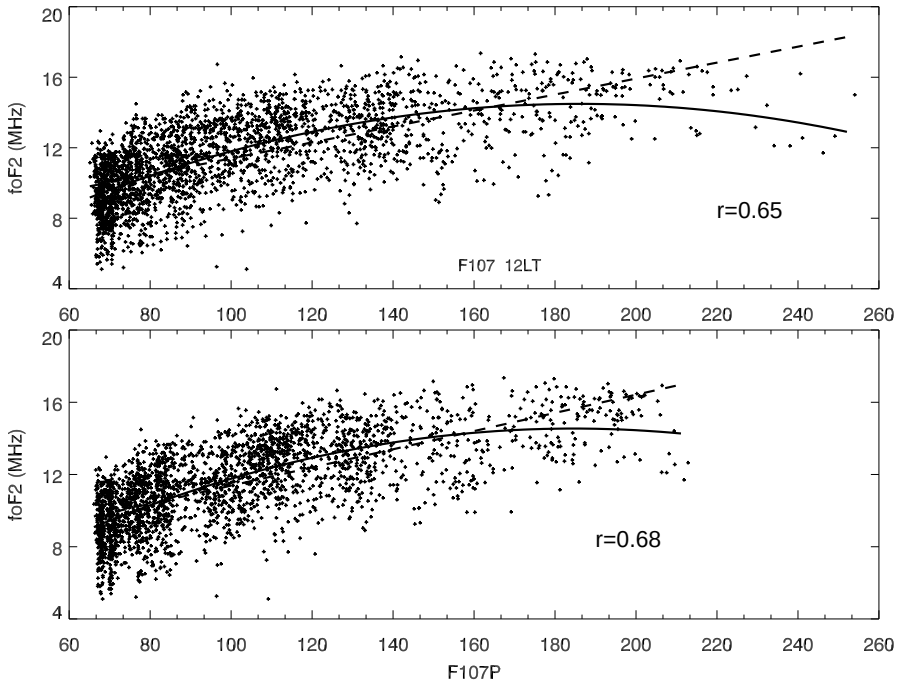

Figure 3. (Top) The responses of the noon foF2 to daily F107 index. The dash and solid lines are the results of linear fitting and 2nd degree polynomial fitting, respectively, and r represents the correlation coefficient. (Bottom) same as figure top, but for the responses of foF2 to F107P index. The solar flux F107 and F107P index unit are 10^{-22} W m^{-2} Hz^{-1} (s.f.u.).

Figure 4 displays diurnal variations of the gradient dfoF2/dF107P (slope), which is obtained with a linear regression, and the correlation coefficients (r) between foF2 and F107P. The lowest value of the correlation coefficient occurs around sunrise with its value greater than 0.6. The slope is lowest around 0500 LT and highest around 2200 LT. The slope is usually lower during daytime than during nighttime. In previous studies, Ratovsky et al. (2014) constructed the local empirical models based on digisonde data over Hainan, Irkutsk, and Norilsk during 2002-2008. In their Figure 2, they presented the diurnal-seasonal behaviors of the slope P_D, which is calculated by the

technique described in Ratovsky and Oinats (2011). They pointed out that NmF2 over Hainan during night hours is strongly dependent on solar activity. This feature is different from the findings of Lei et al. (2005) in which the slope of dNmF2/dF107P at Millstone Hill is lower during nighttime and larger during daytime. One major factor of this difference may be owed to the different dynamic effects (meridional wind and electric field) over the two stations, where Hainan station lies in geomagnetic low latitude and far-from-pole longitude, whereas Millstone Hill lies in geomagnetic mid latitude and near-pole longitude (e.g., Rishbeth et al., 2000a). Moreover, the different context of solar EUV changes and atmospheric consequences would have some contributions to the difference as explained by Liu et al. (2006b).

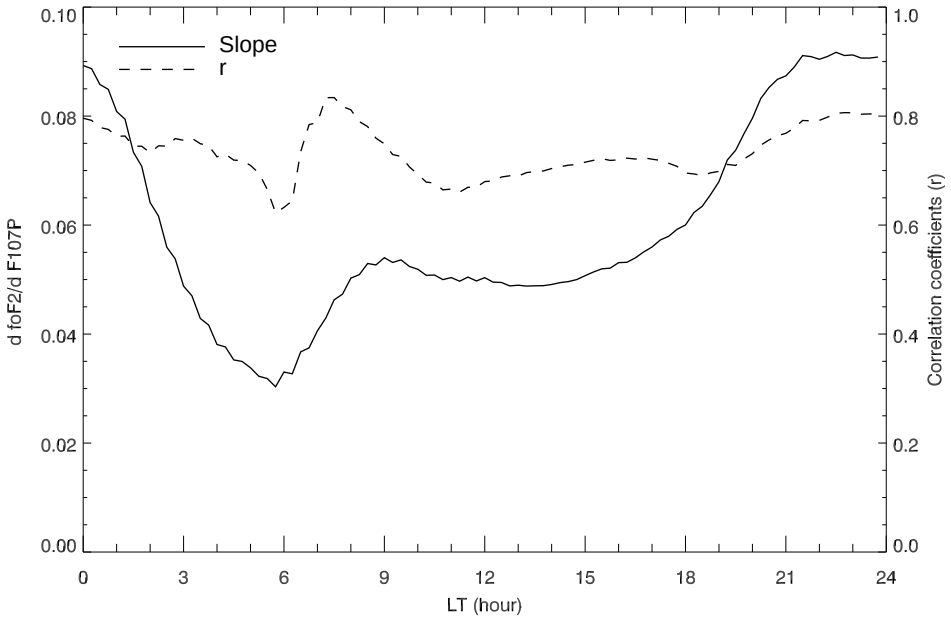

Figure 4. The diurnal variations of the gradient dfoF2/dF107P (slope, unit: MHz per s.f.u.), which is obtained with a linear regression, and the correlation coefficients (r) between foF2 and F107P.

3.2 hmF2 Morphology

For low solar activity, as we can see from Figure 5, hmF2 in autumn shows three minima around 0300, 0700, and 1700 LT. It reaches a diurnal minimum height of 220 km at 0700 LT, and a diurnal peak of 330 km at noontime. The hmF2 in spring varies in a similar way to that in autumn. However, hmF2 in summer and winter varies differently from that in equinoxes. There are two and four minima in hmF2 variations in summer and winter, respectively. The variation of the winter daytime hmF2 exhibits a parabolic shape, with a relatively lower height by ~ 30 km at noontime than that in other seasons. For moderate solar activity, although hmF2 is almost identical to that under low solar activity in the general trend of diurnal variation, it is higher by ~20-50 km at daytime. For high solar activity, there are two outstanding features in hmF2 variations in all seasons. One feature is the pre-reversal enhancement (PRE) phenomenon with abnormal increase of hmF2 near sunset around 1900 LT in equinox and summer, which may be due to the east electric field enhancement near sunset during the high solar activity levels (e.g., Fejer et al., 1991). The other feature is that nighttime hmF2 around midnight exhibits a decreasing trend in high solar

activity, while it shows a peak around midnight in low solar activity. In low solar activity, the peak of hmF2 around midnight may be caused by an increase of upward drifts produced by meridional winds (Kohl and King, 1967), while during the sunrise period, with the beginning of intensive photo-ionization, the layer maximum drops due to rapid production of ionization in the lower F region. In high solar activity, the PRE drift near sunset brings the F2 layer to very high altitude with higher foF2 and lower ions lost rate compared with that in low solar activity. Therefore we can see that the night foF2 in high solar activity is larger than that in low solar activity in Figure 2.

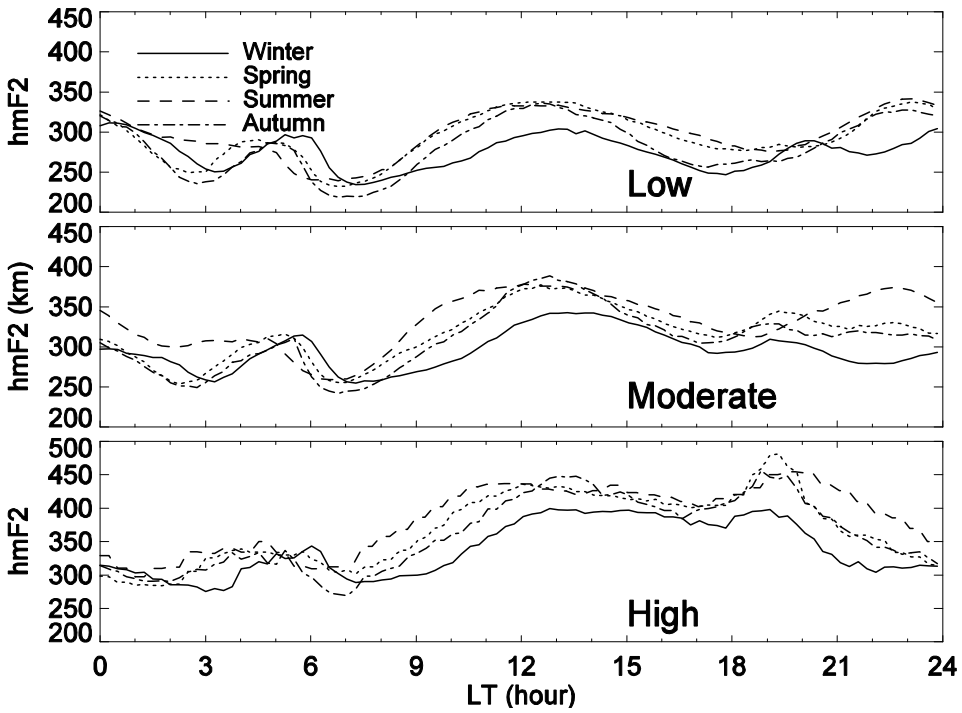

Figure 5. The diurnal and seasonal variation of median hmF2 under low, moderate, and high solar activities.

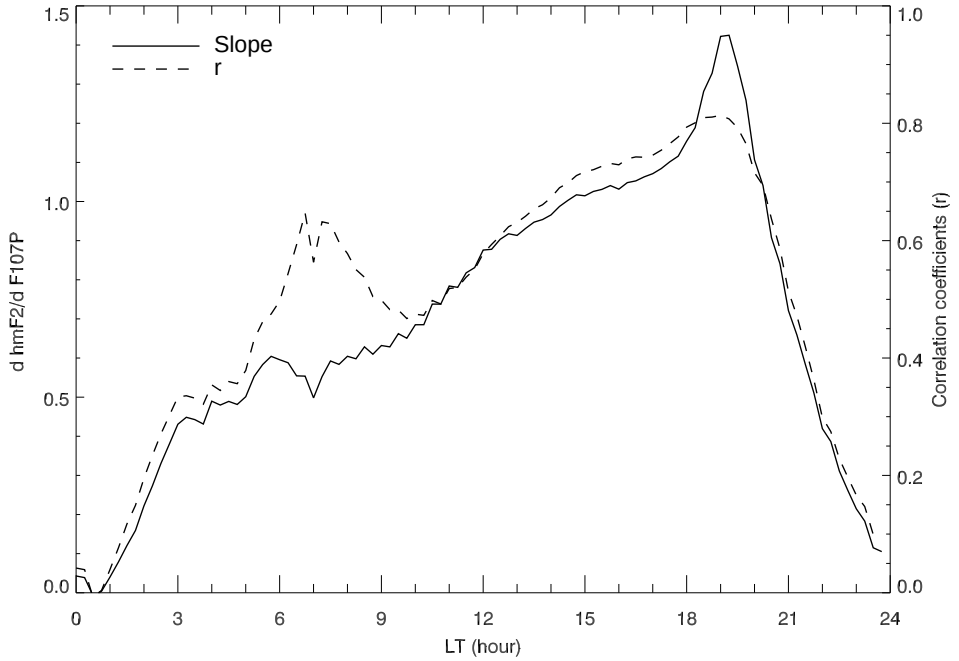

Figure 6. The diurnal variations of the gradient dhmF2/dF107P (slope, unit: km per s.f.u.) and correlation coefficients between hmF2 and F107P in total.

Figure 6 shows the diurnal variations of the gradient dhmF2/dF107P (slope) and correlation coefficients between hmF2 and F107P. The slope quickly increases from midnight to 0300 LT, then generally rises during daytime, suddenly dramatically enhances around 1800 LT and reaches its maximum around 1900 LT, and then drops steeply till midnight. The correlation coefficients are basically greater than 0.5 during daytime and early evening, but they are lower than 0.3 from 2200 to 0300 LT. The trend of the slope variations in all seasons is demonstrated in Figure 7 with greater undulation in their amplitude, but it is similar to the trend of the total variation in figure 6. The daytime hmF2 observed at Hainan increases with increasing solar activity, which is consistent with earlier works (e.g., Rishbeth et al., 2000b; Richards, 2001; Rao et al., 2014). This solar activity dependence of hmF2 is usually explained by the corresponding variation of the neutral temperature and neutral concentrations that control the chemical loss and diffusion balance height and the height of the peak production (Zhang et al., 1999). However, we note that in Figure 7 the slopes turn to little negative values around midnight in equinox seasons, which means the hmF2 decrease slightly with increasing F107P value around midnight over Hainan station. Comparing our results with the slope variations of dhmF2/dF107P at Millstone Hill (referring to Lei et al., 2005, in their figure 6 the slopes are positive and have a diurnal peak at around 1300-1400 LT), there are significant differences between their slopes over two stations around sunset and midnight, which may be due to the different geomagnetic configurations of the two stations.

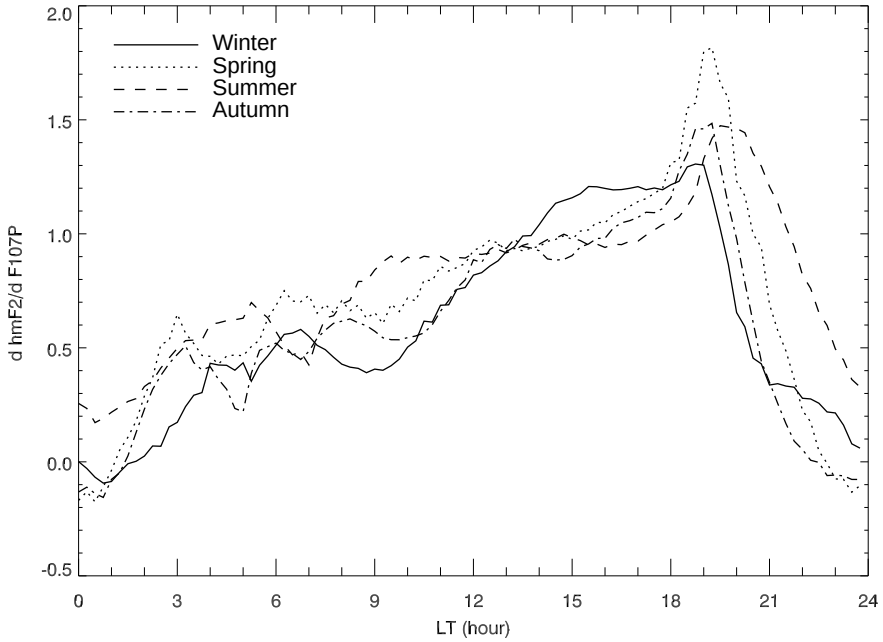

Figure 7. The diurnal variations of the gradient dhmF2/dF107P (slope, unit: km per s.f.u.) in each season.

3.3 Hm morphology

The Chapman scale height (Hm) is a parameter derived from the bottomside profile shape near the F2 peak, when an α-Chapman function is used to extrapolate the topside ionospheric profiles from the information contained in the bottomside ionograms observed by digisonde (Huang and Reinisch, 2001; Reinisch and Huang, 2001). Figure 8 presents the diurnal and seasonal variations of the scale height Hm during different solar activity. In low solar activity, the diurnal variation of Hm has the similar trend in each season; it reaches its peak around sunrise, followed by a sharp drop in the early morning, and then it rises up to its maximum before noon and decreases in the afternoon. There is no appreciable change during nighttime, except for a small peak before midnight in winter. In total, most daytime Hm values between 0700 LT and 1800 LT are higher in summer and lower in winter; while nighttime Hm values exhibit less seasonal variation. The trend of the diurnal and seasonal variations of Hm at Hainan station is basically similar to Wuhan station (30.6° N, 114.4° E) (Liu et al., 2006a), but different from that at Millstone Hill (Lei et al., 2005). For example, in summer, Hm at Hainan station has a notable diurnal variation with a maximum around 1000 LT and a minimum around 0300 LT. At Wuhan station Hm maximizes around 1000 LT but with a minimum around midnight. At Millstone Hill Hm maximizes around 1600 LT and minimizes around midnight. In moderate and high solar activity, the trend of diurnal and seasonal variations of Hm is similar to that in low solar activity, while the value of Hm is generally higher about 5-25 km as compared to that in low solar activity.

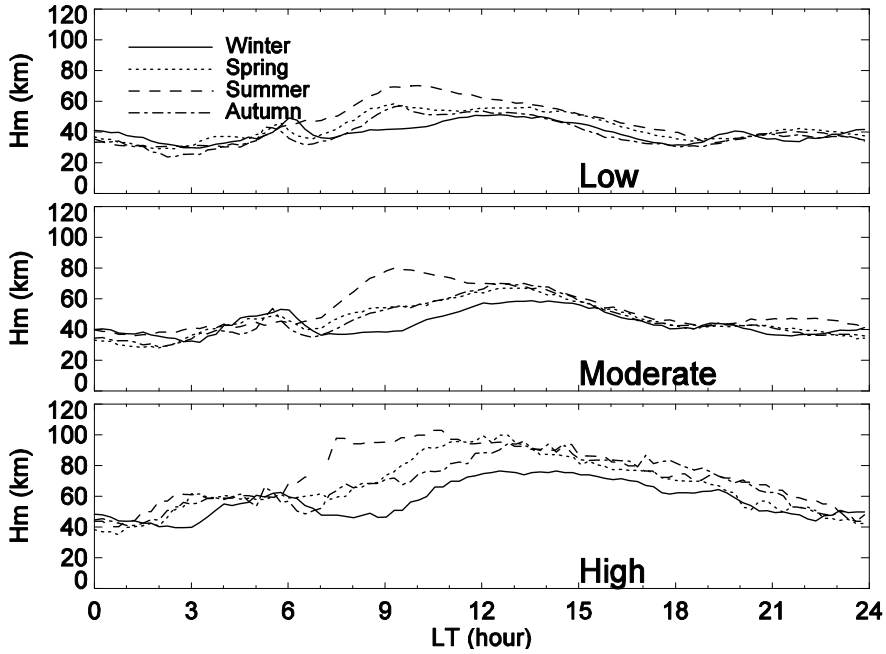

Figure 8. The diurnal and seasonal variations of the scale height Hm during the different solar activity

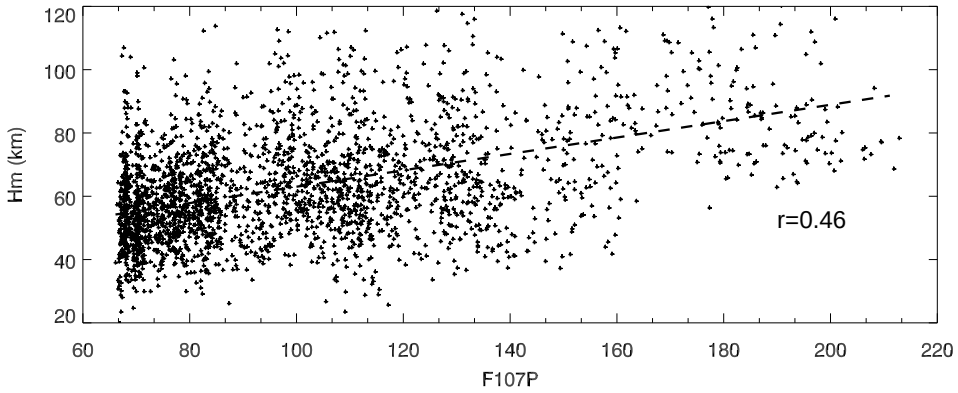

Figure 9. Scatter plots of Hm agaist F107P at 1200 LT and the trend of linear regression (dash line) with their correlation coefficient (r).

Figure 9 gives a scatter plot of Hainan Hm with F107P at 1200 LT and the trend of linear regression with the correlation coefficients. We can see that Hm rises as F107P increases with r value of 0.46. It is evident that Hm is influenced by solar activity. Figure 10 demonstrates the gradient dHm/dF107P (slope) against LT and their r values. Between 1100 and 2100 LT, the r values are greater than 0.4 and the dHm/dF107P are above 0.15 km per solar flux unit. At other local time, most of the r values are lower than 0.4. Figure 11 illustrates the slope against LT in four seasons. The slope is larger in equinox and is lower in winter from 1000 LT to 1900 LT, while during other periods it is generally larger in summer than in other seasons. It is noted that the rate of change is zero or negative around 0900 LT and midnight in winter. These results are very different from those at Wuhan and Millstone Hill (Lei et al., 2005; Liu et al., 2006a), in which all slopes are positive. The basic reason maybe lies in the station location difference, where Hainan station is located on south side of north equatorial ionization anomaly (EIA), but Wuhan

station and Millstone Hill situate on north side of north EIA or mid latitude. The detailed mechanisms of the differences need to be explained in the future by combining the modeling.

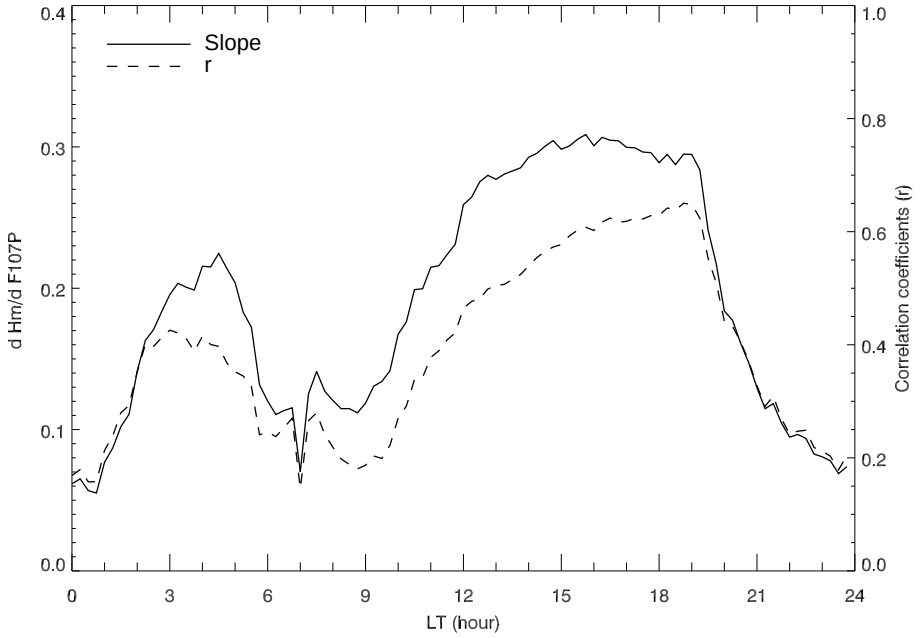

Figure 10. The gradient dH m /d F107P (slope, unit: km per s.f.u.) against LT in total and their r values.

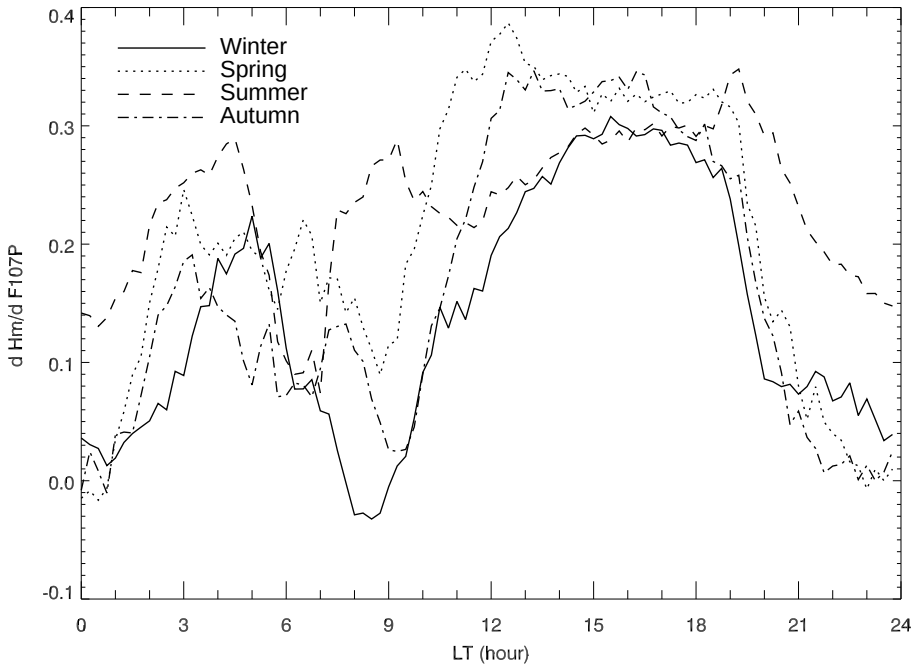

Figure 11. The gradient dHm/dF107P (slope, unit: km s.f.u.) against LT in four seasons.

The scatterplots of Hm versus foF2, hmF2, and the IRI bottomside thickness parameter B0 at Hainan local noon and midnight are given in the left and right panels of Figure 12, respectively. We can see from Figure 12 that Hm shows a strong correlation with B0, a moderate positive correlation with hmF2 and a weak or poor correlation with foF2. Furthermore, Figure 13 shows the correlation coefficient variations between Hm and B0 (also hmF2, foF2) at all local times over

Hainan. The correlation coefficient between Hm and B0 is as high as 0.8-0.97. Actually, the ionogram derived Hm is a measure of the slope of the topside electron number density profile with a Chapman function by (Huang and Reinisch, 2001). So both Hm and B0 are dependent on the shape of the electron density profile in the F region. Thus, these dependences warrant the strong correlation between them. Reinisch et al. (2004) showed the possibility to calculate Hm from the IRI parameters B0 and B1, together with foF2 and hmF2 on the bottomside profile, and then deduced an estimate of the topside profile. Our result supports the idea that future modeling of the topside ionospheric shape is constructed only based on the established B0 parameter set, as suggested before Zhang et al. (2006). This method is a convenient way and would be helpful for improving the IRI topside profile prediction.

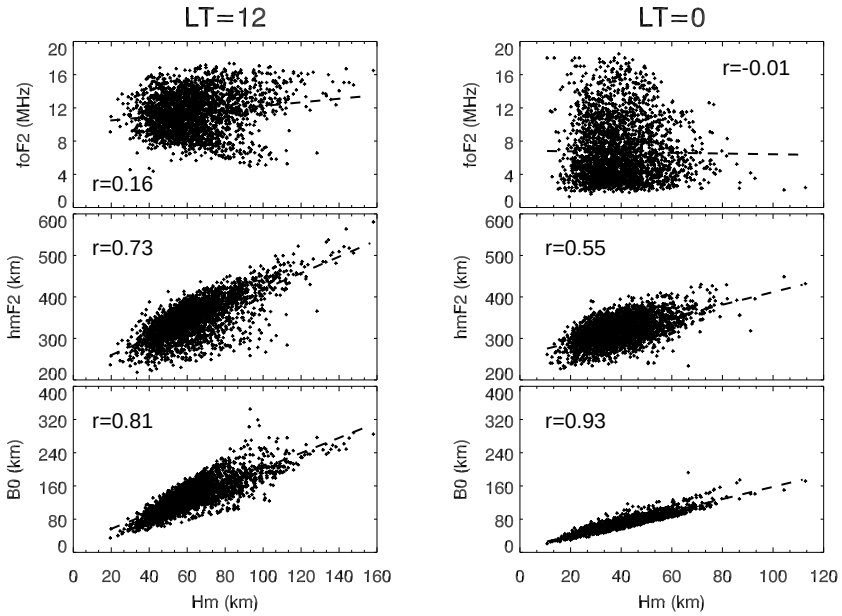

Figure 12. Scatter plots of Hm versus foF2, hmF2, and the best fitted IRI-parameter B0 at Hainan local noon (left) and midnight (right).

The moderate positive correlation between Hm and hmF2 implies that the physical processes that control the variation of hmF2 may also be responsible for that of Hm. It is well known that hmF2 mainly depends on the neutral winds and electric fields. For example, Liu et al. (2006a, in their Figure 8) showed the meridional neutral wind obtained by HWM93 over Wuhan had a similar sine form annual pattern as shown in hmF2 and Hm during daytime. While during nighttime in their annual variations, the neutral wind keeps a regularly sine form undulation, but Hm does not have that obvious sine form undulation. So there was a significant difference between the neutral wind and Hm in nighttime. Lee and Reinisch (2007) pointed out that the r value between Hm and hmF2 at geomagnetic equatorial station Jicamarca was high (r=0.7-0.9) and suggested the Hm variations would be affected by vertical drift velocity associated with equatorial electric field. How these factors affect Hm over Hainan station deserves further study for us through combining the neutral wind and electric field models in the low latitude region.

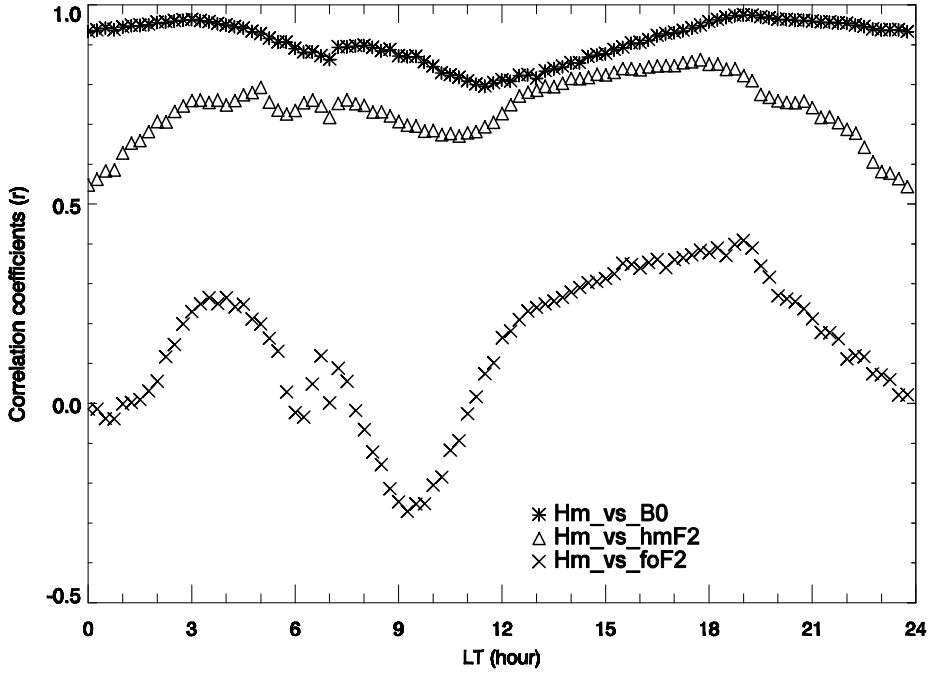

Figure 13. The diurnal variations of correlation coefficients between Hm and B0, hmF2, foF2 at all local time at Hainan station.

3.4 Comparison with IRI

International Reference Ionosphere (IRI) model is one of the most widely utilized empirical models for the determination of ionospheric behavior (e.g., Bilitza and Reinisch, 2008; Bilitza et al, 2011). Previous studies have shown that the IRI model generally reproduces well prediction results compared to that of observations in foF2 over low and mid latitude station, while the modeled hmF2 values in some seasons are significantly different from the observed ones (Wang, et al., 2009; Rao, et al., 2014). Figure 14 shows the diurnal variations of the seasonal median differences between IRI-2012 predicted foF2 and observed ones in the different solar activity, and their corresponding percentage variations, where both the difference and the percentage are defined as $\Delta foF2=foF2_{predicted}-foF2_{observed}$ and $P_{\Delta foF2}(\%) = (foF2_{predicted}-foF2_{observed})/foF2_{observed} \times 100\%$. Since the period during 2008-2010 is extremely low solar activity period, we mark the period as the "Very Low" in Figure 14. From Figure 14 (a), we can see that the each seasonal median difference of foF2 mainly increases with increasing solar activity. In particular, the differences are comparatively large around 1900 LT in spring under (very) low solar activity, at night time in equinox under moderate solar activity, and around midnight in each season under high solar activity. From Figure 14 (b), we can see that the percentage of foF2 differences has the similar variation patterns with different magnitudes compared to the corresponding foF2 differences. The outstanding feature of the percentage of foF2 difference exhibits the largest magnitude before dawn, which may be due to the smaller background observed values. The detailed statistical mean and standard deviation of the seasonal median difference and their corresponding percentage are listed in Table 1 and Table 2. On the whole, their means are negative and their standard deviations are larger as solar activity changes from low to high levels. In other words, IRI predicted foF2 values are basically lower than observed ones (underestimated), and the magnitude of their deviations increase significantly as solar activity level increases.

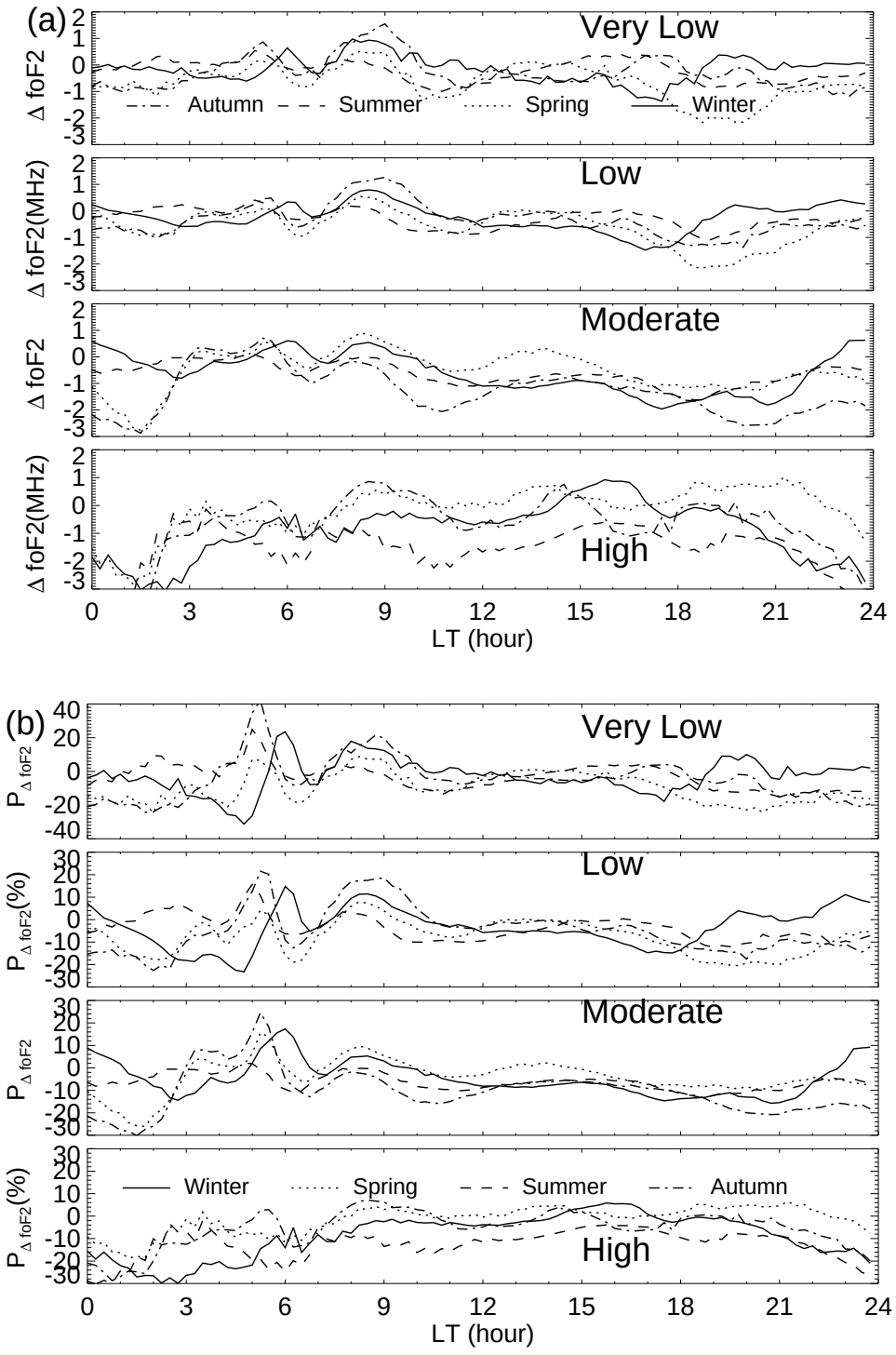

Figure 14. The diurnal variations of the seasonal median differences between IRI-2012 predicted foF2 and observed ones under the different solar activity in the plots (a) and their corresponding Percentages in the plots (b).

Table 1. The mean (left column) and standard deviation (right column) of seasonal median differences between IRI predicted foF2 and observed ones (unit: MHz)

Solar activity	Winter	Spring	Summer	Autumn
Very low	−0.2,0.5	−0.7,−0.7	−0.2,0.4	−0.3,0.6
Low	−0.2,0.5	−0.6,0.7	−0.3,0.4	−0.3,0.6
Moderate	−0.6,0.8	−0.5,0.8	−0.6,0.4	−1.3,0.9
High	−0.9,1.0	−0.2,0.9	−1.6,0.9	−0.7,1.1

Table 2. The mean (left column) and standard deviation (right column) of the percentage of the seasonal median differences between IRI predicted foF2 and observed ones (unit: %)

Solar activity	Winter	Spring	Summer	Autumn
Very Low	−2.7,9.9	−9.7,8.9	−3.1,7.5	−4.0,12.5
Low	−3.4,8.6	−7.8,7.8	−3.8,5.6	−4.8,10.1
Moderate	−4.6,7.8	−3.9,7.8	−6.2,3.6	−10.3,10.1
High	−8.9,9.6	−1.7,6.2	−12.7,6.7	−5.6,8.2

As far as hmF2 comparison are concerned, Wang et al. (2009) have shown that the IRI predicted hmF2 using CCIR M(3000)F2 option are in poor agreement with the observed ones, but the IRI predicted hmF2 using the measured M(3000)F2 inputs are in very good agreement with the observed ones. These points are supported further by our examination. We show the diurnal variations of the seasonal median differences between IRI-2012 predicted hmF2 using the measured M(3000)F2 inputs and the observed ones under different solar activity in Figure 15 (a), and the corresponding percentage variations in Figure 15 (b). The detailed statistical means and standard deviations of their differences and the corresponding percentage variations are listed in Table 3 and 4, respectively. In general, under very low, low and moderate solar activity (Figure 15), the predicted hmF2 agree quite well with observations at all local time in each season and the deviations between them are usually within 20 km. Under high solar activity, however, the standard deviations between them in each season are obviously magnified about 1.5 times than those under the low and moderate solar activity (seen in Table 3). The percentage variations of their differences in Figure 15 (b) have the similar patterns with the corresponding variations of their differences. The deviations of the percentage variations are basically within 10% and 15% under low-moderate and high solar activity, respectively. Their standard deviations also increase as solar activity increases from low-moderate level to high level (referring to Table 4). It can be shown from the bottom panels of Figure 15 (a) and (b) that the undulation of the differences obviously increases dramatically under high solar activity.

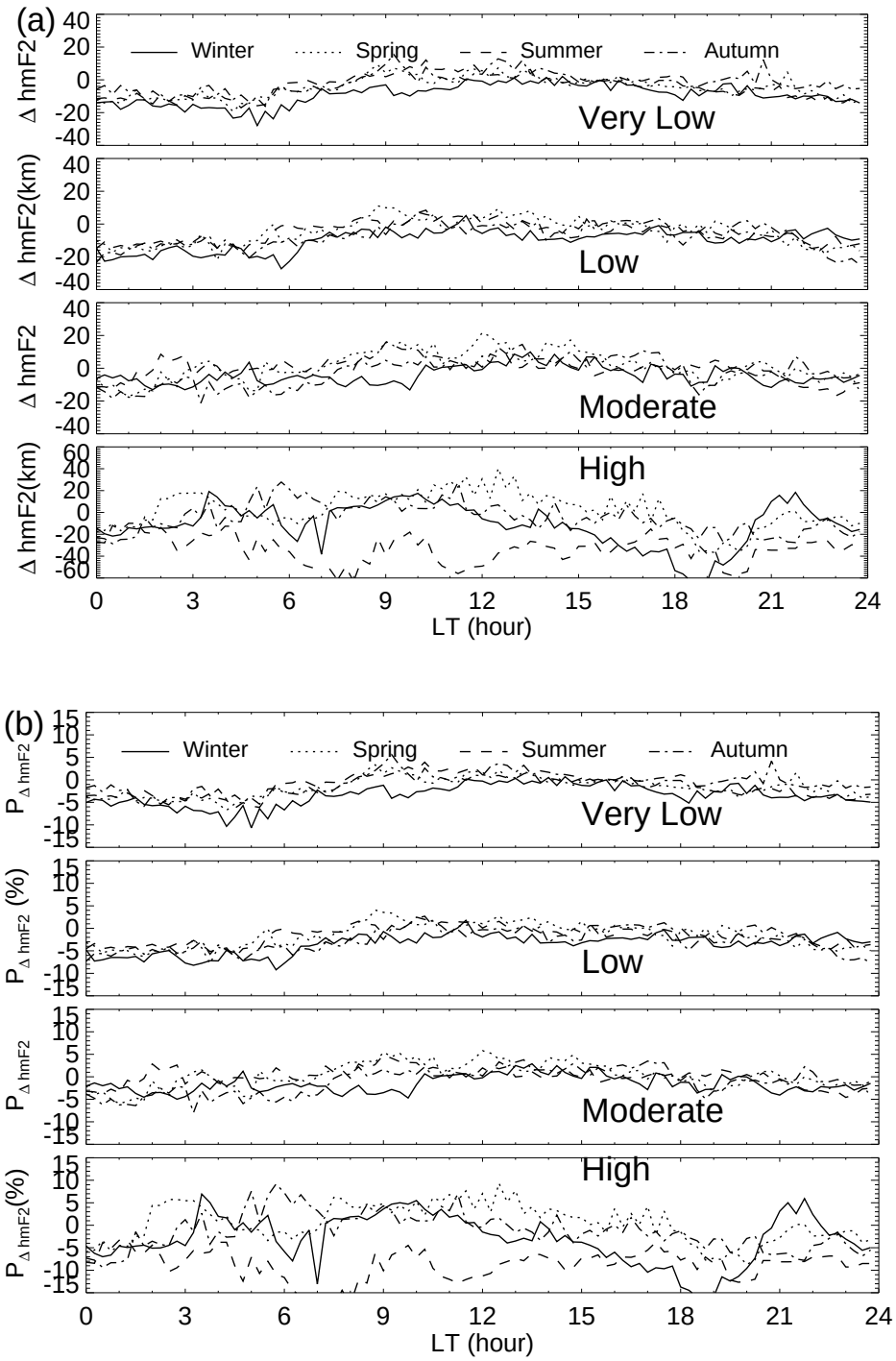

Figure 15. The diurnal variations of the seasonal median differences between IRI-2012 predicted hmF2 using the measured M(3000)F2 inputs and the observed ones under the different solar activity in the plots (a) and their corresponding Percentages in the plots (b). where Δ hmF2=$hmF2_{predicted}$ –$hmF2_{observed}$ and $P_{\Delta hmF2}$ (%) = ($hmF2_{predicted}$ –$hmF2_{observed}$) /$hmF2_{observed}$ × 100%. Here "Very Low" refers to the period during 2008-2010.

Table 3. The mean (left column) and standard deviation (right column) of seasonal median differences between IRI predicted hmF2 and observed ones (unit: km)

Solar activity	Winter	Spring	Summer	Autumn
Very Low	−9.1,6.4	−4.5,6.3	−3.7,7.0	−1.7,6.4
Low	−9.9,6.3	−4.5,7.8	−4.7,6.2	−7.2,7.4
Moderate	−4.2,5.4	1.3,9.0	0.2,6.5	−2.6,8.6
High	−11.3,19.0	1.9,16.5	−33.3,12.3	−4.8,13.7

Table 4. The mean (left column) and standard deviation (right column) of the percentage of the seasonal median differences between IRI predicted hmF2 and observed ones (unit: %)

Solar activity	Winter	Spring	Summer	Autumn
Very Low	−3.4,2.4	−1.6,2.2	−1.3,2.4	−0.7,2.3
Low	−3.5,2.2	−1.6,2.7	−1.6,2.1	−2.6,2.5
Moderate	−1.5,1.9	0.3,2.8	0,1.9	−1.0,2.8
High	−3.0,5.4	0.5,4.2	−8.6,3.2	−1.3,4.0

In brief, we first made the quantitative comparison between the observed foF2/hmF2 over Hainan and the ones predicted by IRI-2012 during the period of a solar cycle. The results have shown that the IRI predicted foF2 values are basically underestimated and the magnitude of its deviations clearly increases as increasing solar activity. The IRI predicted hmF2 obtained with measured M(3000)F2 inputs in low and moderate solar activity agree well with the observed ones. However, their deviations in high solar activity are significantly magnified.

4. Summary

This paper utilized the whole solar activity cycle data observed by a digisonde at Hainan station during the low to moderate geomagnetic activity period from 2002 to 2012 to investigate the diurnal, seasonal, and annual variations of foF2, hmF2 and Chapman scale height Hm and their dependences on the solar activity, as well as firstly to make some quantitative comparison with IRI-2012 modeling results. The conclusions can be drawn as follows:

(1) The winter anomaly in the daytime foF2 appears in different levels of solar activity. The duration of the adjacent values around daytime peak of foF2 in each season are noticeably extended as increasing solar activity. The semiannual anomaly in the daytime and nighttime foF2 with two maxima in equinox seasons is present. The foF2 values exhibit a close correlativity with a solar activity factor F107P and the correlation coefficients in their diurnal variations are around 0.7. The slope of foF2 varying with F107P is usually lower during daytime than that during nighttime.

(2) The afternoon and evening hmF2 values show a good correlation with F107P (their correlation coefficients more than 0.6), but at other times hmF2 is not well correlated with F107P. The prominent character of hmF2 at sunset in equinox and summer seasons under high solar activity period has a clear increase, which may be due to strong pre-reversal enhancement. For the first time, it is found that hmF2 around midnight decreases with increasing F107P index in equinox seasons.

(3) The diurnal variation of Hm usually has two peaks around noontime and pre-sunrise. The daytime Hm has an annual variation with maximum in summer and minimum in winter.

Although the daytime Hm depends on solar activity, the correlation coefficient between them is not large due to meridional wind, and other factors.

(4) The IRI predicted foF2 values are basically underestimated and the magnitude of their deviations clearly increases with increasing solar activity. The IRI predicted hmF2 obtained with measured M(3000)F2 inputs in low and moderate solar activity agree well with the observed ones. However, their deviations in high solar activity are significantly magnified.

(5) These results are considerably different from those reported over Millstone Hill (Lei et al, 2005), which may be mainly due to the different dynamic effect (meridional wind and electric field) and different geomagnetic configuration over the low latitude station Hainan and middle latitude station Millstone Hill.

Acknowledgements. The Ap and F107 indices are downloaded from the SPIDR website http://spidr.ngdc.noaa.gov. The IRI-2012 model has been obtained from the website http://IRI.gsfc.nasa.gov. We acknowledge the use of data from the Chinese meridian Project. The digisonde data used are available upon request (G. J. Wang, gjwang@nssc.ac.cn) and downloaded partly from the website http://www.meridianproject.ac.cn. This work was supported by the National Natural Science Foundation of China (41574150, 41474137, 41674145) and the Specialized Research Fund for State Key Laboratories of China.

References.

Abdu, M.A., 2005. Equatorial ionosphere-thermosphere system: electrodynamics and irregularities. Adv. Space Res., 35, 771–787.

Adler, N. O., Elias, A. G., Manzano, J. R., 1997. Solar cycle length variation: Its relation with ionospheric parameters. J. Atmos. Sol. Terr. Phys., 59(2), 159 – 162.

Balan, N., Bailey, G. J., Jenkins, B., Rao, P. B., Moffett, R. J., 1994a. Variations of ionospheric ionization and related solar fluxes during an intense solar cycle. J. Geophys. Res., 99(A2), 2243–2253.

Balan, N., Bailey, G. J., Moffett, R. J., 1994b, Modeling studies of ionospheric variations during an intense solar cycle. J. Geophys. Res., 99(A9), 17,467–17,475.

Bilitza, D., Reinisch, B., 2008. International reference ionosphere 2007: improvements and new parameters. Adv. Space Res. 42 (4), 599–609.

Bilitza, D., McKinnell, L. A., Reinisch, B., Fuller-Rowell, T., 2011. The international reference ionosphere today and in the future. J. Geod., 85, 909-920. DOI 10.1007/s00190-010-0427-x.

Fejer, B.G., de Paula, E.R., Gonzalez, S.A., Woodman, R.F., 1991. Average vertical and zonal F region plasma drifts over Jicamarca. J. Geophys. Res. 96, 13,901–13,906.

Fuller-Rowell, T. J., 1998. The “thermospheric spoon”: a mechanism for the semi-annual density variation. J. Geophys. Res., 103, 3951-3956.

Haralambous, H., Oikonomou, C., 2015. Comparison of peak characteristics of the F2 ionospheric layer obtained from the Cyprus Digisonde and IRI-2012 model during low and high solar activity period. Adv. Space Res., 56, 1927-1938.

Hinteregger, H. E., Fukui,K., Gilson, B. R., 1981. Observational, reference and model data on solar EUV, from measurements on AE-E. Geophys. Res. Lett., 8, 1147-1150.

Huang, X., Reinisch, B. W., 2001. Vertical electron content from ionograms in real time. Radio Sci., 36(2), 335–342.

Kane, R. P., 1992. Sunspots, solar radio noise, solar EUV and ionospheric foF2. J. Atmos. Terr. Phys., 54,

463–466.

Kawamura, S., Balan, N., Otsuka, Y., Fukao, S., 2002. Annual and semiannual variations of the midlatitude ionosphere under low solar activity. J. Geophys. Res., 107(A8), 1166, doi:10.1029/2001JA000267.

Kohl, H., King, J. W., 1967. Atmospheric winds between 100 and 700 km and their effects on the ionosphere. J. Atmos. Terr. Phys., 29, 1045–1062.

Laštovička, J., Mikhailov, A. V., Ulich, T., Bremer, J., Elias, A. G., Ortis de Adler, N., Jara, V., Abarca del Rio, R., Foppiano, A. P., Ovalle, E., Danilov, A. D., 2006. Long-term trends in *fo*F2: A comparison of various methods. J. Atmos. Solar-Terr. Phys., 68, 1854–1870.

Lee, C.C., Reinisch, B.W., 2006. Quiet-condition hmF2, NmF2, and B0 variations at Jicamarca and comparison with IRI-2001during solar maximum. J. Atmos. Sol. Terr. Phys. 68 (18), 2138–2146.

Lee, C.-C., Reinisch, B. W., 2007. Quiet-condition variations in the scale height at F2-layer peak at Jicamarca during solar minimum and maximum. Ann. Geophys., 25(12), 2541– 2550.

Lei, J., Liu, L., Wan, W., Zhang, S.-R., 2005. Variations of electron density based on long-term incoherent scatter radar and ionosonde measurements over Millstone Hill. Radio Sci., 40, RS2008, doi:10.1029/2004RS003106.

Liu, L., Wan, W., Ning, B., 2006a. A study of the ionogram derived effective scale height around the ionospheric hmF2. Ann. Geophys., 24(3), 851– 860.

Liu, L., Wan, W., Ning, B., Pirog, O. M., Kurkin, V. I., 2006b, Solar activity variations of the ionospheric peak electron density. J. Geophys. Res., 111, A08304, doi:10.1029/2006JA011598.

Liu, L., Le, H., Wan, W., Sulzer, M. P., Lei, J., Zhang, M.-L., 2007. An analysis of the scale heights in the lower topside ionosphere based on the Arecibo incoherent scatter radar measurements. J. Geophys. Res., 112, A06307, doi:10.1029/2007JA012250.

Liu, L., He, M., Wan, W., Zhang, M.-L., 2008. Topside ionospheric scale heights retrieved from Constellation Observing System for Meteorology, Ionosphere, and Climate radio occultation measurements. J. Geophys. Res., 113, A10304,doi:10.1029/2008JA013490.

Ma, R., Xu, J., Liao, H., 2003. The features and a possible mechanism of semiannual variation in the peak electron density of the low latitude F2 layer. J. Atmos. Sol. Terr. Phys., 65, 47 – 57, doi:10.1016/S1364-6826(02)00192-X.

Millward, G. H., Moffett, R. J., Quegan, S., Fuller-Rowell, T. J., 1996. Ionospheric F2 layer seasonal and semiannual variations. J. Geophys. Res., 101, 5149–5156, doi:10.1029/95JA03343.

Mikhailov, A. V., Mikhailov, V. V., 1995. Solar cycle variations of annual mean noon foF2. Adv. Space Res., 15(2), 79– 82

Mosert, M., Buresova, D., Magdaleno, S., de la Morena, B., Altadill, D., Ezquer, R. G., Scida, L., 2012. An analysis of the scale height at the *F*2-layer peak over three middle-latitude stations in the European sector. Earth Planets Space, 64, 493-503.

Nambala, F. J., McKinnell, L.-A., Oyeyemi, E., 2008. Variations in the ionospheric scale height parameter at the F2 peak over Grahamstown. South Africa, Adv. Space Res., 42, 707–711.

Qian, L., Burns, A. G., Solomon, S. C., Wang, W., 2013. Annual/semiannual variation of the ionosphere. Geophys. Res. Lett., 40, 1928–1933, doi:10.1002/grl.50448.

Rao S. S., Sharma, Shweta, Galav, P., Pandey, R., 2014. Variation of monthly mean foF2 and hmF2 over a mid latitude station during the period 1997-2006. Adv. Space Res., 53, 744-751. Doi.org/10.1016/j.asr.2013.12.018

Ratovsky, K.G., Oinats, A.V., 2011. Local empirical model of ionospheric plasma density derived from digisonde measurements at Irkutsk. Earth Planets Space, 63 (4), 351–357.

Ratovsky, K.G., Oinats, A.V., Medvedev, A.V., 2009. Diurnal and seasonal variations of F2 layer characteristics over Irkutsk during the decrease in solar activity in 2003–2006: Observations and IRI-2001 model predictions.

Adv. Space Res., 43 (11), 1806–1811.

Reinisch, B. W., Huang, X., 2001. Deducing topside profiles and total electron content from bottomside ionograms. Adv. Space Res., 27(1), 23– 30, doi:10.1016/S0273-1177(00)00136-8.

Reinisch, B. W., Huang, X., Belehaki, A., Shi, J., Zhang, M., Ilma, R., 2004. Modeling the IRI topside profile using scale height from groundbased ionosonde measurements. Adv. Space Res., 34, 2026 – 2031, doi:10.1016/j.asr.2004.06.012.

Richards, P. G., 2001. Seasonal and solar cycle variations of the ionospheric peak electron density: Comparison of measurement and models. J. Geophys. Res., 106(A12), 12,803–12,819.

Richards, P. G., Torr, D. G., Reinisch, B. W., Gamache, R. R., Wilkinson, P. J., 1994. F2 peak electron density at Millstone Hill and Hobart: Comparison of theory and measurement at solar maximum. J. Geophys. Res., 99(A8), 15,005–15,016.

Rishbeth, H., Setty, C. S. G. K., 1961. The F layer at sunrise. J. Atmos. Terr. Phys., 10, 263–276.

Rishbeth, H., 1998. How the thermospheric circulation affects the ionosphere. J. Atmos. Sol. Terr. Phys., 60, 1385– 1402, doi:10.1016/S1364-6826(98)00062-5.

Rishbeth H., Müller-Wodarg, I. C. F., Zou, L., Fuller-Rowell, T. J., Millward, G. H., Moffett, R. J., Idenden, D. W., Aylward, A. D., 2000a. Annual and semiannual variations in the ionospheric F2-layer: II. Physical discussion. Ann. Geophysicae, 18, 945-956.

Rishbeth, H., Sedgemore-Schulthess, K. J. F., Ulich, T., 2000b. Semiannual and annual variations in the height of the ionospheric F2-peak. Ann. Geophysicae, 18, 285-299.

Rishbeth H., (2004), Questions of the equatorial F2-layer and thermosphere, J. Atoms. Sol. Terr. Phys., 66, 1669-1674.

Torr, M. R., Torr, D. G., 1973. The seasonal behaviour of the F1 layer of the ionosphere. J. Atmos. Terr. Phys. 24, 1126 – 1140.

Wang X., Shi, J. K., Wang, G. J., Gong, Y., 2009. Comparison of ionospheric F2 peak parameters foF2 and hmF2 with IRI2001 at Hainan. Adv. Space Res. 43, 1812-1820.

Yu, T., Wan, W., Liu, L., Zhao, B., 2004. Global scale annual and semiannual variations of daytime NmF2 in the high solar activity years. J. Atmos. Sol. Terr. Phys., 66, 1691– 1701.

Zhang, M.L., Shi, J.K., Wang, X., Wu, S.Z., Zhang, S.R., 2004. Comparative study of ionospheric characteristic parameters obtained by DPS-4 digisonde with IRI2000 for low latitude station in China. Adv. Space Res. 33 (6), 869–873.

Zhang, M.-L., Reinisch, B.W., Shi, J. K., Wu, S. Z., Wang, X., 2006. Diurnal and seasonal variation of the ionogram-derived scale height at the F2 peak. Adv. Space Res., 37, 967– 971, doi:10.1016/j.asr.2006.02.004.

Zhang, M.L., Shi, J.K., Wang, X., Shang, S.P., Wu, S.Z., 2007. Ionospheric behavior of the F2 peak parameters foF2 and hmF2 at Hainan and comparisons with IRI model predictions. Adv. Space Res. 39 (5), 661–667.

Zhang, S.-R., Fukao, S., Oliver, W. L., Otsuka, Y., 1999. The height of the maximum ionospheric electron density over the MU radar. J. Atmos. Sol. Terr. Phys., 61, 1367–1383.

Zou, L., Rishbeth, H., Müller-Wodarg, I. C. F., Aylward, A. D., Millward, G. H., Fuller-Rowell, T. J., Idenden, d. W., Moffett, R. J., 2000. Annual and semiannual variations in the ionospheric F2-layer: I. Modelling. Ann. Geophysicae, 18, 927-944.